Effects of micron-scale zero valent iron on behaviors of antibiotic resistance genes and pathogens in thermophilic anaerobic digestion of waste activated sludge

Title: Effects of micron-scale zero valent iron on behaviors of antibiotic resistance genes and pathogens in thermophilic anaerobic digestion of waste activated sludge

Authors: Wenqian Li[a], Lina Pang[a, *], Efthalia Chatzisymeon[b], Ping Yang[a]

[a.] College of Architecture and Environment, Sichuan University, Chengdu 610065, P.R. China

[b.] School of Engineering, Institute for Infrastructure and Environment, The University of Edinburgh, Edinburgh EH9 3JL, United Kingdom

∗**Corresponding author:** Lina Pang (panglina@scu.edu.cn)

Abstract:

This work investigated the metagenomics-based behavior and risk of antibiotic resistance genes (ARGs), and their potential hosts during thermophilic anaerobic digestion (TAD) of waste activated sludge, enhanced by micron-scale zero valent iron (mZVI). Tests were conducted with 0, 25, 100, and 250 mg mZVI/g total solids (TS). Results showed that up to 7.3% and 4.8% decrease in ARGs' abundance and diversity, respectively, were achieved with 100 mg mZVI/g TS. At these conditions, ARGs with health risk in abundance and human pathogenic bacteria (HPB) diversity were also decreased by 8.3% and 3.6%, respectively. Additionally, mZVI reduced abundance of 72 potential pathogenic supercarriers for ARGs at high health risk by 2.5%, 5.0%, and 6.1%, as its dosage increased. Overall, mZVI especially at 100 mg/g TS can mitigate antibiotic resistance risk in TAD. These findings are important for better understanding risks of ARGs and their pathogenic hosts in ZVI-enhanced TAD of solid wastes.

Key words: Metagenomics; Health risk; Resistome; Human pathogenic bacteria; Potential pathogenic hosts

1. Introduction

Antibiotic resistance encoded in antibiotic resistance genes (ARGs) is becoming a daunting threat to global "One Health". It is generally accepted that waste activated sludge (WAS) is an important hotspot of multiple and abundant ARGs (Zhang et al., 2022b). Up to 181 ARG subtypes, mainly resistant to multidrug, macrolide-lincosamide-streptogramin (MLS), bacitracin, sulfonamides, and tetracycline, with the highest abundance being 1.57×10^{-1}copies per 16S rRNA gene have been detected in WAS in sewage treatment plants (Yoo et al., 2020). Alarmingly, some of them, even at low abundance, could pose great clinical significance and transmission to the environment via WAS treatment and disposal (Zhang et al., 2022c), which can eventually put human health at risk (Bondarczuk et al., 2016). Moreover, human pathogenic bacteria (HPB), such as *Escherichia coli*, *Vibrio cholerae*, *Streptococcus pneumoniae*, have also been revealed in WAS (Cai & Zhang, 2013; Zhang et al., 2022a). Some of these bacteria can develop multiple antibiotic resistances and are recognized as ARGs' supercarriers (Jang et al., 2019), thus acting as another factor aggravating the antibiotic resistance crisis (Lin et al., 2022). These thereby indicate the pressing need to comprehensively understand the health risk of ARGs in the WAS treatment process in addition to ARGs' abundance and types, if the current prevailed antibiotic resistance crisis is to be mitigated.

Thermophilic anaerobic digestion (TAD) has been proven to be a promising technology for WAS reduction, energization, and pollution control (Gao et al., 2017). Meanwhile, as previously reported, TAD can create a favorable environment to eliminate the abundance of ARGs (Diehl & Lapara, 2010), but there is no consistent conclusion, due to the

different WAS properties and surveillance approaches that have been studied (Jang et al., 2019; Tian et al., 2016; Zhang et al., 2015). Moreover, WAS with high microbial and chemical densities can facilitate the spread of ARGs in TAD processes (Zhang et al., 2011). Many reports have also demonstrated that the microbial community and physicochemical properties of WAS can vary and shift the behavior of ARGs and their hosts during anaerobic digestion (AD). These shifts are often triggered by the changes in AD conditions, such as temperature (Xu et al., 2020), or the presence of exogenous substances (Jang & Kan, 2022; Pang et al., 2022), which are commonly applied to enhance the performance of TAD. Therefore, there is a risk that ARGs and their hosts would be affected by these TAD enhancers, but this has been barely studied until now.

Recently, micron zero valent iron (mZVI) has attracted widespread interest as a cost-effective agent in improving methane production in AD of food waste (Jing et al., 2022), swine manure (Yang et al., 2018b), and glucose-substrate (Zhong et al., 2022). Also, it has been observed that mZVI performed well in eliminating ARGs in various AD applications, such as wastewater treatment (Xu et al., 2021b), co-digestion of waste sludge and kitchen waste (Gao et al., 2017), and swine manure treatment (Zhang et al., 2018). However, current investigations on the effect of ZVI on the overall abundance and diversity of ARGs in sludge AD process have mainly focused on nano-sized ZVI (nZVI). Yet, considering the different effects on physiochemical properties and microbial composition induced by ZVI with various particle sizes (Xu et al., 2021a; Zhong et al., 2022), the role of mZVI in the TAD process regarding the entire antibiotic resistome in WAS has not been fully explored.

This work aims to fill this knowledge gap by following a metagenomic approach. Firstly, a full picture of the ARGs profile and microbial community in WAS before and after TAD with different mZVI dosages will be provided. Second, the behavior and risk of ARGs will be elucidated with regards to abundance, diversity, and human health-based impacts using current assessment frameworks (Zhang et al., 2022c), as well as prioritizing HPB with or without mZVI. Finally, the potential pathogenic hosts for high risk ARGs will be identified to explore the antibiotic resistance risk in WAS in the presence of mZVI. Findings of this work will be fundamentally important to promote an understanding of the potential effect of mZVI on TAD treatment of solid wastes containing ARGs and opportunistic pathogens.

2. Materials and methods

2.1 Substrate and additive

WAS collected from a municipal sewage treatment plant in Chengdu, China, was settled at 4°C before use. Its physicochemical properties are listed in Table 1. mZVI (150 μm, 99% metals basis) was purchased from Macklin Reagent Co. Ltd., China.

2.2 Experimental design

Four batch experimental groups spiked with 0, 25, 100, and 250 mg mZVI/g TS and marked as Z0, Z1, Z2, and Z3, respectively, were digested for 32-day in serum bottles with working volume of 200 mL. WAS with 8% (w/v) TS were added in each serum bottle, then sealed with rubber stoppers and incubated at 55(±1)°C in a water bath after being flushed with high-purity nitrogen for 2 min. WAS samples collected at the end of TAD experiments in Z0, Z1, Z2, and Z3 groups were centrifuged at 8,000 rpm for 10 min. From

these, the supernatant was filtered through a 0.45 μm membrane for measuring the physicochemical properties, and sediments along with raw WAS (marked as Raw) were stored at -80°C for metagenomic analysis. Gas samples were collected using air bags (300 mL) for measuring daily and cumulative biogas and methane productions. Duplicate experiments (n=2) were also carried out in parallel.

2.3 DNA extraction and metagenomic sequencing

DNA from raw WAS and sediment samples from the experimental groups were extracted using Fast DNA Spin Kit for Soil (MP Biomedicals, USA). DNA from the same operational conditions were mixed for one sequencing sample. Genomic DNA was then detected by 1% agarose gel electrophoresis.

Shotgun metagenome sequencing was performed using the Illumina MiSeq (Illumina Inc., USA) with PE150 strategy at Majorbio Bio-Pham Technology Co., Ltd. (Shanghai, China). 6-gigabytes data was created for each sample. Raw sequences were qualified and then trimmed to remove low-quality reads by fastp (https://github.com/OpenGene/fastp). The reads were filtered by BWA. Then clean reads for each sample were assembled into contigs (the minimum contig length ≥ 300 bp) using MEGAHIT (https://github.com/voutcn/megahit) with default settings. Open reading frames (ORFs) within contigs were subsequently predicted using MetaGene (http://metagene.cb.k.u-tokyo.ac.jp/) (Pang et al., 2022), and genes with nucleic acid length ≥100 bp were selected and translated into amino acid sequences. Details about the assembly and prediction of ORFs are presented (see supplementary material). A non-redundant gene catalogue (gene sequence cluster similarity (Identity) ≥ 0.9, gene sequence clustering coverage (Coverage)

≥ 0.9), was obtained by CD-HIT (http://www.bioinformatics.org/cd-hit/) (Zhang et al. 2022c). The comparison of the high-quality reads from each sample with the non-redundant gene set (95% identity) was performed using the SOAPaligner (http://soap.genomics.org.cn/, v 2.21).

2.4 Antibiotic resistance genes annotation, normalization, and risk assessment

ARGs were annotated against the comprehensive antibiotic resistance database (CARD, v 3.0.9) using Diamond (http://www.diamondsearch.org/index.php, v 0.8.35). The abundance (coverage, times per Giga base, ×/Gb) of ARGs was defined using Eq. (1) (Xiong et al., 2018):

$$\text{Abundance (coverage, ×/Gb)} = \sum_{1}^{n} \frac{N_{i\ (reads)} \times \frac{L_{i\ (reads)}}{L_{\ (ARG-like\ ORFs)}}}{S} \quad (1)$$

where n is the number of the annotated ARG-like ORFs belonging to that ARG type or subtype; N_i *(reads)* is the number of the reads mapped to the ARG-like ORFs; L_i *(reads)* is the length of the Illumina sequencing reads (bp); *L (ARG-like ORFs)* is the length of the target ARG-like ORFs (bp); S is the size of the sequencing data after quality control (Gb).

The health risk of annotated ARGs was evaluated based on the database provided by Zhang et al. (2022c), which includes four ranked risks for 2561 ARG subtypes considering their human accessibility, mobility, pathogenicity, and clinical availability. Thereinto, the ARGs at risk were classified into 4 levels, with Q1 ranked as the highest risk, followed by Q2, Q3, and Q4.

2.5 Microbial characterization and human pathogenic bacteria identification

Microbial composition was characterized by NR database (v 20200604) using BLASTP via Diamond software (http://ab.inf.uni-tuebingen.de/software/diamond/). The prioritized HPB were identified according to A-to-Z database from the National Infection Prevention and Control Manual.

2.6 Chemical analyses

Total solids (TS), volatile solids (VS), soluble chemical oxygen demand (SCOD), soluble proteins (SP), soluble polysaccharides (SC), ammonium-nitrogen (NH_4^+-N), biogas and methane productions, pH, and volatile fatty acids (VFAs) including acetic acid, propionic acid, butyric acid, and iso-butyric acid were measured according to previous studies (Lu et al., 2022b; Qi et al., 2021). Total iron was determined by atomic absorption spectrometer (WFX-810, Beijing Rayleigh Analytical Instrument Co., Ltd., China), and ferrous iron was characterized by phenanthroline spectrophotometry.

2.7 Statistical analysis

SPSS 21.0 and Origin 2022b were used for statistical analysis and processing. Significant differences ($p < 0.05$) between groups were assessed by Fisher's exact test. The correlation was analyzed by Spearman linear correlation ($R>0.85$, $p<0.05$). Network visualization was conducted on the platform of Gephi (v 0.9.7).

2.8 Availability of data

The metagenomics data was deposited into the National Center for Biotechnology Information (NCBI) sequence read archive database (SRA) (Accession Number: PRJNA914103).

3. Results and discussion

155 **3.1 Performance of thermophilic anaerobic digestion (TAD)**

156 Biogas and methane production, and characteristics of WAS before (Raw) and after TAD
157 treatment with different dosages of mZVI are listed in Table 1. These results indicated
158 that TAD performances varied significantly between groups without (Z0) and with mZVI
159 (Z1, Z2, and Z3) in terms of methane (biogas) production, SCOD, SC, NH_4^+-N, and VFAs
160 content. For example, cumulative methane yield in groups with mZVI (Z1, Z2, and Z3)
161 was 1.7, 12.0, and 12.0 times higher than in Z0, respectively. Moreover, in groups with
162 mZVI, concentrations of iso-butyric acid and pH were positively correlated with the
163 dosage of mZVI. In addition, Z2 and Z3 performed similarly but better than Z1 in methane
164 and biogas production, and this could be confirmed by the observed decrease in
165 concentrations of SCOD, SC, acetic and butyric acids, as well as substrates for methane
166 and biogas yield, in Z2 and Z3. Overall, an up to 12-fold increase of methane yield
167 enhanced by mZVI was obtained in this study. This improvement was higher than those
168 (35.9% - 44.5% promotions) observed previously in mesophilic AD. This might be
169 attributed to the fact that although mZVI could enhance the release of substrates for
170 methane production, and the activity of key enzymes involved in the AD process (Jing et
171 al., 2022; Liang et al., 2021), the substrate properties and operational temperature would
172 also affect the AD performance (Xu et al., 2020).

173 [**Table 1**]

174 **3.2 Fate of antibiotic resistance genes**

175 **3.2.1 Abundance and diversity of antibiotic resistance genes**

176 The profile of total ARGs in raw WAS and in TAD treated with different dosages of mZVI

177 included 877 known subtypes within 21 types (Fig. 1a and Fig. 1b). Of these, the
178 dominant ARG type of multidrug resistance genes (relative abundance of 37.4%) was
179 followed by glycopeptide (12.1%), tetracycline (11.7%), MLS (10.4%), and peptide
180 (8.3%) resistance genes. However, the most diverse ARG type was genes resistant to beta-
181 lactam (225 subtypes), followed by multidrug (184 subtypes), aminoglycoside (92
182 subtypes), and MLS (87 subtypes), respectively. Moreover, the top three resistance
183 mechanisms for all ARGs were antibiotic efflux (62.5%), antibiotic target alteration
184 (20.6%), and antibiotic target protection (7.7%), respectively (see supplementary
185 material).
186 ARG types of multidrug, glycopeptide, tetracycline, and MLS were prevalent in TAD
187 treated sludge with and without mZVI. This is consistent with previous findings in sewage
188 treatment plants (Li et al., 2015). This might be attributed to the fact that these antibiotics
189 were widely used in human activities (Singh et al., 2019). Multidrug resistance genes
190 were the most abundant in this study possibly due to the dominant resistance mechanism
191 of antibiotic efflux, which could provide defense against several inhibitory constituents,
192 including multidrug resistance (Christgen et al., 2015).
193 The total abundance of ARGs were 12329, 14962, 14592, 13949, and 14465 ×/Gb in raw
194 WAS and the four TAD experimental groups (Fig. 1b). It can be observed that TAD could
195 enrich ARG abundance no matter whether mZVI is present or not, and the highest
196 enrichment occurred in Z0. Although many studies demonstrated that TAD performs
197 better in driving a sharp decline in the total abundance of ARGs (Diehl & Lapara, 2010;
198 Jang et al., 2019; Tian et al., 2016), this was not the case in this study, since only a

199 decrease in diversity was obtained. This phenomenon might be attributed to the fact that
200 the fate and profile of ARGs could vary due to the different AD conditions, substrates
201 properties, and applied surveillance approaches, like qPCR, which also limited the
202 understanding of the change of ARGs' diversity in AD process (Xu et al., 2020; Zhang et
203 al., 2011).
204 The addition of mZVI could mitigate the enrichment by TAD, except ARGs in types of
205 nucleoside and fusidic acid. Notably, mZVI at 100 mg/g TS proved best in mitigating the
206 risk of ARGs by reducing their abundance, since the abundances of 15 ARG types were
207 decreased to the lowest level in Z2. Furthermore, Venn analysis (Fig. 1c) showed that 621
208 ARG subtypes were shared among raw and the four treated WAS, with the number of
209 respective unique ARG subtypes being 52, 9, 7, 3, and 4. The diversity of ARG subtypes
210 in raw WAS could be reduced by TAD treatment from 800 to 761 in Z0, and this reduction
211 was further improved to 747, 726, and 728 when the mZVI dosages increased and so were
212 the unique ARG subtypes.
213 [**Figure 1**]
214 The presence of mZVI, especially at 100 mg/g TS (Z2), was found effective in improving
215 methane production and in mitigating ARGs risk by total abundance and diversity of
216 ARGs in the TAD process (Z0), and this was dosage independent. Such performance was
217 consistent with previous findings that have demonstrated a correlation between a decrease
218 in ARGs' abundance and an increase in methane production (Lu et al., 2022a). Besides,
219 current studies on the response behavior of ARGs to mZVI in TAD are mainly focused
220 on certain types of antibiotic resistance. For example, regarding the widely studied

tetracycline-resistant genes, qPCR results showed that ZVI (40 μm) at 60 g/L were beneficial for eliminating *tetA*, *tetG*, *tetM*, *tetO*, *tetC*, and *tetX* but without great differences from those at 5 g/L in TAD (50°C) of WAS and kitchen waste (Gao et al., 2017). In this study, similar reductions, compared with Z0, in the abundance of 14 tetracycline ARGs including *tetX* were also achieved by mZVI (Z1-Z3). Meanwhile, the total abundance of other 46 genes resistant to tetracycline was reduced by 0.5% and 3.3% in Z1 and Z2, while being slightly enriched in Z3. This could be explained by the release of ferrous iron at certain concentrations, like 5.5 μg/mL in Z2 in this study. This effect can significantly alter the dynamics of functional genes, including ARGs, and exert various selection pressures on them, thereby shifting their abundance and composition (Gao et al., 2017; Lu et al., 2022a). Notably, some ARGs rebounded with mZVI in the TAD treatment compared to those in raw WAS, such as *APH(3')-IIb*, *OXA-1*, *tet(E)*, and *PER-2*, and this was probably due to the fact that mZVI can perform well in directly affecting ARGs themselves instead of inactivating their hosts (Zhang et al., 2020).

3.2.2 Health risk assessment of antibiotic resistance genes

The public health concern was prioritized in this study by focusing on clinically relevant ARGs and their potential to transfer to humans, thereby driving the evolution of antibiotic-resistant pathogens (Zhang et al., 2022c). 350 ARG subtypes were identified at health risk (see supplementary material), and the ARG subtypes in Q1 (highest risk), Q2, Q3, and Q4 were 128, 68, 62, and 92, occupying 50.9%, 12.8%, 13.5%, and 22.8%, respectively, in total abundance of 43311 ×/Gb (Fig.2). In consistence with the behavior of all ARGs, the abundance of these ARGs at risk was also increased across the TAD

process from 7751 ×/Gb (raw WAS) to 9238 ×/Gb (Z0), which dropped to 8971, 8533, and 8819 ×/Gb, respectively in Z1, Z2, and Z3. While, the diversity of risky ARGs in raw WAS (328) decreased in TAD (Z0, 324), and was further reduced in the presence of mZVI (319 in Z1, 321 in Z2, and 309 in Z3). This suggested that the abundance and diversity of all ARGs at risk increased in Z0, while it was reduced in mZVI-enhanced TAD (Z1-Z3) with the best performance observed at 100 mg mZVI/g TS (Z2).

Regarding the 128 ARG subtypes at high risk (Q1), they could be classified mainly in genes resistant to multidrug (74), tetracycline (16), and aminoglycoside (13). Their abundance in raw WAS (4042 ×/Gb, 123 subtypes) was also enriched in Z0 (4677 ×/Gb, 123 subtypes), and mZVI could decrease this to 4530 (120 subtypes), 4319 (125 subtypes), and 4496 ×/Gb (125 subtypes), respectively. This indicated that mZVI at all three concentrations could further mitigate the risk of ARGs in Q1 by abundance. However, only the addition of 25 mg mZVI/g TS improved their diversity reduction. These results suggest that mZVI exerts an overall positive effect in relieving the abundance and diversity of ARGs at risk, but for those at high risk it depends on the dosage of mZVI (Xu et al., 2021a).

[**Figure 2**]

To be more specific, among 123 ARG subtypes in Q1 in raw WAS, the abundance of 62 ARG subtypes decreased in the absence of mZVI (Z0), and 44 of these 62 ARG subtypes were further reduced in abundance with mZVI (Z1, Z2, and Z3). Also, abundances of ARGs like *evgA*, *arlS*, *evgS* reduced the most by up to 65.1 ×/Gb (Z1), 48.9 ×/Gb (Z1), and 43.9 ×/Gb (Z1), respectively.

Moreover, 11 ARG subtypes at risk that existed in raw WAS were not detected in the four TAD treatment groups. In addition, *gadW* (Q1) and *dfrF* (Q2) encoding resistance to multidrug and diaminopyrimidine, decreased from 0.9 and 0.6 ×/Gb in raw WAS, to 0.3 and 0.5 ×/Gb, respectively, in Z0 (after TAD treatment). However, these genes were not detected in the other three mZVI groups. Notably, 9 risky ARG subtypes that were not detected in raw WAS and Z0, such as *AAC(3)-Iidc* (aminoglycoside, Q1), *OXA-1* (beta-lactam, Q1), *tet(E)* (tetracycline, Q2), *PER-2* (beta-lactam, Q2) were enriched in groups with mZVI.

It should be noted that 350 ARGs at risk were revealed including 134 multidrug resistance genes, 74 of which were found in 128 high risk ARGs (Q1), accounting for the majority of ARGs at (high) risk. Such high health risk induced by ARGs for multidrug could be due to the fact that they can render multiple antibiotics, even those with clinical importance, inefficient and/or invalid, while further triggering severe mortality (Christgen et al., 2015).

3.3 Taxonomic overview of microbial community

3.3.1 Diversity and composition of microbial community

Microbial taxonomy was annotated regarding the raw and TAD treated sludge with different dosages of mZVI (Fig.3). The predominant bacterial phyla were Proteobacteria (relative abundance of 40.7%), Actinobacteria (22.8%), and Chloroflexi (17.5%) regardless of treatment condition (Fig. 3a). The high prevalence of these three phyla was also detected in previous AD studies (Li et al., 2021; Zhao et al., 2022), since AD microbes have been reported to play a role in carbohydrate degradation, which could

promote the performance of AD (Rivière et al., 2009). Additionally, bacterial genera were dominated by *Candidatus_Promineofilum* (5.1%), *Dechloromonas* (2.9%), and *Coprothermobacter* (2.2%) (Fig. 3b-f).

[**Figure 3**]

The top three dominant phyla (relative abundance > 1%) in the four experimental groups were the same but with different relative abundances (Fig. 3g). It can be seen that, compared to raw WAS, the TAD treatment (Z0) increased these three dominant phyla significantly, and reduced the abundances of phyla Bacteroidetes (from 13.9% to 1.6%), Nitrospirae (from 4.6% to 1.2%), and Acidobacteria (from 3.7% to 1.1%). This reduction was further enhanced by mZVI (Z1-Z3). However, the presence of mZVI showed the potential to enrich phylum Chloroflexi compared with raw WAS and Z0, and its dosage was found to be positively correlated with its relative abundances.

The relative abundances in total of 27 classified genera (with total relative abundance > 0.3%) increased after the TAD treatment (from 15.8% in Raw to 29.3% in Z0), but fluctuated slightly with mZVI (27.8%, 31.2%, and 29.4% in Z1, Z2, and Z3, respectively) (Fig. 3h). Among these 27 genera, 4 of them showed a decrease in relative abundance after the TAD process, while *Nitrospira* and *Candidatus_Competibacter* decreased further as the dosage of mZVI increased. 23 genera were enriched in Z0 compared to raw WAS. Interestingly, only 4 genera (*Candidatus_Promineofilum*, *Nocardioides*, *Marmoricola*, and *Microbacterium*) were further increased with mZVI, while 9 genera like *Dechloromonas* and *Candidatus_Accumulibacter* were reduced by mZVI, especially at 100 mg /g TS.

For archaea, the relative abundance of all 7 classified genera (with total relative abundance > 0.3%) increased during the TAD treatment (from 49.8% in Raw to 61.7% in Z0), and even further with mZVI (62.5%, 89.8%, and 89.9% in Z1, Z2, and Z3) (see supplementary material). Among them, *Methanothermobacter* (0.1% in Raw) was significantly increased in TAD by 9.1% (Z0), and further cumulated by up to 10.1%, 70.6%, and 54.8% with mZVI. Besides, the enrichment of *Methanosarcina* was also observed with mZVI (2.4% in Z0, and 2.5-15.7% in Z1-Z3).

Generally, the genus *Candidatus_Promineofilum* (phylum Chloroflexi), followed by *Dechloromonas* (phylum Proteobacteria), and *Coprothermobacter* (phylum Coprothermobacter) were predominant in both raw WAS and TAD treated sludge groups. Their relative abundances were enriched in TAD (Z0), but only the first genus could be further enriched in the presence of mZVI regardless of its dosage. As previously reported, *Dechloromonas* has the ability to degrade organic matters via electron transfer (Yang et al., 2015), and *Coprothermobacter* can hydrolyze protein and take part in thermophilic syntrophic interaction with hydrogenotrophic methanogenic archaea (Gagliano et al., 2014). Also, *Candidatus_Promineofilum* is capable of generating energy by respiration or by carbohydrate fermentation (like sugar) in AD (Tandishabo et al., 2012). Additionally, *Methanothermobacter*, as the dominant thermophilic hydrogenotrophic methanogen, and *Methanosarcina*, as the acetoclastic methanogen (Barros et al., 2017), were enhanced by the application of mZVI. These indicated that mZVI could enhance the hydrogenotrophic and acetoclastic methanogenic pathway probably via promoting hydrolysis and fermentation of carbohydrates.

3.3.2 Profiles of human pathogenic bacteria

A total of 98 HPB species in 61 genera were obtained and their distribution in raw WAS, Z0, Z1, Z2, and Z3 were 93 (relative abundances of 0.4%), 87 (0.5%), 89 (0.5%), 84 (0.5%), and 88 (0.5%), respectively (see supplementary material). Specifically, HPB species of *Pseudomonas aeruginosa*, *Propionibacterium* species, and *Pseudomonas* spp. persisted in raw WAS and four TAD groups, with relative abundance > 10.0%, recognized as core HPB. Besides, the most abundant 30 HPB are illustrated in Fig. 4a. Compared to the raw WAS, the relative abundance of only 7 HPB species, *Acinetobacter baumannii*, *Bacillus anthracis*, *Brevundimonas diminuta*, *Brevundimonas vesicularis*, *Chlamydia trachomatis*, *Citrobacter* spp., and *Corynebacterium diphtheriae*, could be decreased by mZVI, but this was dosage-independent.

[**Figure 4**]

Interestingly, mZVI (Z1-Z3) could decrease the relative abundance of superbugs, such as *Pseudomonas aeruginosa*, *Klebsiella pneumoniae* MDR, and *Acinetobacter baumannii* in TAD (Z0), while not being effective in eliminating *Enterococcus faecalis*. Such positive inhibitory effects on superbugs, like *Pseudomonas aeruginosa*, were also found in nZVI application (Anbouhi et al., 2019), probably due to its particle size and its role on the cell wall of Gram-negative bacteria. Furthermore, the observed increase in the relative abundance of *Enterococcus faecalis* in this study could be attributed to the hydrogen-producing capacity of the genus *Enterococcus* (Yang & Wang, 2022), which have been enhanced by mZVI (Jing et al., 2022).

3.4 Relationships between human pathogenic bacteria and antibiotic resistance

genes

In addition to the health risk induced by ARGs themselves, their bacterial hosts, especially the pathogenic ones, can trigger the clinical inefficacy or invalidity of antibiotics, thereby posing a threat to human health. Potential hosts at the genus level with relative abundance in total > 0.3%, as predominant genera, were explored for 128 high risk ARGs (Q1) (Fig. 4b). The co-occurrence network consisted of 131 nodes and 588 edges, including 27 genera and 104 ARGs in Q1. All 27 genera were significantly positively correlated with 90 high risk ARGs, with 4 genera of *Tetrasphaera*, *Coprothermobacter*, *Nitrospira*, and *Candidatus_Competibacter*, potentially carrying at least 20 ARGs in Q1. Furthermore, genus *Pseudomonas*, a known HPB species, was found as the potential host for 18 ARGs in Q1, like *kdpE*, *efrA*, *bacA*, *YojI*, *mgrA*, and *aadA5*.

Moreover, special attention was paid to how HPB can host potentially high risk ARGs. The co-occurrence pattern between 98 HPB detected and ARGs in Q1, focusing on their positive correlations, was analyzed to determine possible twin risk from pathogens and antibiotic resistance (Fig. 4c). The entire network consisting of 221 nodes and 687 edges, showed that 95 HPB species had significant positive correlations with 126 ARGs at high risk. This indicates serious risks induced by the existence of either ARGs or HPB or both in raw WAS and TAD treated sludge with and without mZVI. Such ARG-carrying HPB have also been uncovered in AD systems of sludge (Ju et al., 2022), the mixture of livestock manure and fruit wastes (Lin et al., 2022), and dairy manure (Jang & Kan, 2022). Of the 95 potential pathogenic hosts, the majority belonged to 35 genera within the phylum Proteobacteria (49 species) and 6 genera within the phylum Firmicutes (20

375 species), both of which were also reported as potential hosts for ARGs (Pang et al., 2022),
376 and acted as opportunistic pathogens (Jang et al., 2019; Lin et al., 2022). Besides, these
377 two phyla play a vital role in hydrolytic acidification as the core community (Zhao et al.,
378 2022). This may be the reason why pathogens were enriched in the TAD process. The
379 abundance of HPB affiliated with these two phyla increased from 72.2% in raw WAS to
380 78.5% in Z0, but was mitigated by mZVI treatment. In addition, this alleviation was
381 enhanced as dosages of mZVI increased (77.1%, 76.0%, 74.6% in Z1, Z2, Z3). These
382 suggest that mZVI can relieve the propagation risk of ARGs, and this effect was dosage
383 dependent.
384 Thereinto, 15 ARGs had significant positive correlations with at least 10 HPB, and 10 of
385 these 15 ARGs were resistant to multidrug. Remarkably, 72 species were recognized as
386 potential supercarriers for at least 3 ARGs, and their relative abundance was increased in
387 TAD treatment (from 73.0% in Raw to 79.2% in Z0), and reduced with mZVI (77.2%,
388 75.2%, and 74.4% in Z1-Z3, respectively). This implies the dosage-dependent mitigation
389 effect of mZVI on the risk of possible simultaneous pathogenicity and antibiotic
390 resistance in TAD. Besides, *Acinetobacter baumannii*, *Chlamydia trachomatis*,
391 *Francisella tularensis*, and *Providencia stuartii* co-occurred with at least 20 ARGs at high
392 risk, respectively.
393 It is noteworthy that *Acinetobacter baumannii* was a clinical superbug, and that the 23
394 high risk ARGs it hosted were resistant to multidrug (13 subtypes), tetracycline (6),
395 aminoglycoside (2), fluoroquinolone (1), and MLS (1). Most importantly, 5 other
396 superbugs, namely *Enterobacter cloacae*, *Klebsiella pneumoniae* MDR, *Pseudomonas*

aeruginosa, *Staphylococcus aureus*, and *Enterococcus faecalis*, were also detected, and they were positively correlated with 13, 7, 4, 4, and 1 ARGs, respectively. Among these ARGs, both *tet(40)* and *MexK* were highly associated with *Enterobacter cloacae* and *Staphylococcus aureus* in the meantime, and *poxtA* co-occurred with *Staphylococcus aureus* and *Klebsiella pneumoniae* MDR simultaneously. Furthermore, except for *Enterococcus faecalis*, there were 5 supercarriers that hosted a total of 47 ARGs (Q1). These genes were mainly resistant to multidrug (29), tetracycline (9), aminoglycoside (3), and MLS (3). Similar superbug hosts were also revealed in the report through metagenome-assembled genomes (Zhang et al., 2022c). For example, *Klebsiella pneumoniae* MDR was recognized as the host for *acrB*, *adeF*, which is consistent with the findings of this study. *Enterococcus faecalis* could acquire *IsaA*, whereas it was found to co-occur with *ErmA*. The inconsistency may be because mZVI/TAD changed the ARGs' hosts. Therefore, an in-depth investigation should be carried out to explore how ARGs at high risk can be transferred among HPB, especially superbugs, and even to humans during the TAD treatment of WAS regarding mitigation of their environmental and health risks.

4. Conclusion

The comprehensive profiles of ARGs in terms of abundance, diversity, health risk, and potential pathogenic hosts in WAS before and after the TAD treatment with different mZVI dosages were investigated. Results showed that mZVI, especially at 100 mg/g TS could mitigate the risk of ARGs by abundance and diversity in TAD. Such effect was also observed in abundance of ARGs at (high) health risk and diversity of HPB. Finally, the increased abundance in TAD of 72 HPB, as supercarriers for ARGs at high health risk,

could be alleviated by the presence of mZVI and be positively depended on its dosage.

E-supplementary data for this work can be found in e-version of this paper online

Acknowledgements

This study was supported by the Regional Innovation cooperation Project of Science and Technology Department of Sichuan Province (Grant No. 2022YFQ0036).

References

1. Anbouhi, T.S., Esfidvajani, E.M., Nemati, F., Haghighat, S., Sari, S., Attar, F., Pakaghideh, A., Sohrabi, M.J., Mousavi, S.E., Falahati, M. 2019. Albumin binding, anticancer and antibacterial properties of synthesized zero valent iron nanoparticles. Int. J. Nanomed., 14, 243-256.

2. Barros, V.G.d., Duda, R.M., Vantini, J.d.S., Omori, W.P., Ferro, M.I.T., Oliveira, R.A.d. 2017. Improved methane production from sugarcane vinasse with filter cake in thermophilic UASB reactors, with predominance of *Methanothermobacter* and *Methanosarcina* archaea and Thermotogae bacteria. Bioresour. Technol., 244, 371-381.

3. Bondarczuk, K., Markowicz, A., Piotrowska-Seget, Z. 2016. The urgent need for risk assessment on the antibiotic resistance spread via sewage sludge land application. Environ. Int., 87, 49-55.

4. Cai, L., Zhang, T. 2013. Detecting human bacterial pathogens in wastewater treatment plants by a high-throughput shotgun sequencing technique. Environ. Sci. Technol., 47(10), 5433-5441.

5. Christgen, B., Yang, Y., Ahammad, S.Z., Li, B., Rodriquez, D.C., Zhang, T., Graham, D.W. 2015. Metagenomics shows that low-energy anaerobic−aerobic treatment reactors

441 reduce antibiotic resistance gene levels from domestic wastewater. Environ. Sci. Technol.,
442 49(4), 2577-2584.
443 6. Diehl, D.L., Lapara, T.M. 2010. Effect of temperature on the fate of genes encoding
444 tetracycline resistance and the integrase of class 1 integrons within anaerobic and aerobic
445 digesters treating municipal wastewater solids. Environ. Sci. Technol., 44(23), 9128-9133.
446 7. Gagliano, M.C., Braguglia, C.M., Rossetti, S. 2014. *In situ* identification of the
447 synthrophic protein fermentative *Coprothermobacter* spp. involved in the thermophilic
448 anaerobic digestion process. FEMS Microbiol. Lett., 358(1), 55-63.
449 8. Gao, P., Gu, C., Wei, X., Li, X., Chen, H., Jia, H., Liu, Z., Xue, G., Ma, C. 2017. The
450 role of zero valent iron on the fate of tetracycline resistance genes and class 1 integrons
451 during thermophilic anaerobic co-digestion of waste sludge and kitchen waste. Water Res.,
452 111, 92-99.
453 9. Jang, H.M., Choi, S., Shin, J., Kan, E., Kim, Y.M. 2019. Additional reduction of
454 antibiotic resistance genes and human bacterial pathogens via thermophilic aerobic
455 digestion of anaerobically digested sludge. Bioresour. Technol., 273, 259-268.
456 10. Jang, H.M., Kan, E. 2022. Enhanced removal of antibiotic resistance genes and
457 human bacterial pathogens during anaerobic digestion of dairy manure via addition of
458 manure biochar. Chemosphere, 304, 135178.
459 11. Jing, H., Cui, Y., Ye, M., Yan, X., Liu, Y. 2022. Effect of zero-valent iron on
460 acidification and methane production using food waste under different food-to-
461 microorganism ratios. Renewable Energy, 198, 131-143.
462 12. Ju, F., Li, B., Ma, L., Wang, Y., Huang, D., Zhang, T. 2016. Antibiotic resistance

463 genes and human bacterial pathogens: Co-occurrence, removal, and enrichment in
464 municipal sewage sludge digesters. Water Res., 91, 1-10.
465 13. Li, B., Yang, Y., Ma, L., Ju, F., Guo, F., Tiedje, J.M., Zhang, T. 2015. Metagenomic
466 and network analysis reveal wide distribution and co-occurrence of environmental
467 antibiotic resistance genes. The ISME Journal, 9(11), 2490-2502.
468 14. Li, J., Chen, T., Yin, J., Shen, D. 2021. Effect of nano-magnetite on the propionic
469 acid degradation in anaerobic digestion system with acclimated sludge. Bioresour.
470 Technol., 334, 125143.
471 15. Liang, J., Luo, L., Li, D., Varjani, S., Xu, Y., Wong, J.W.C. 2021. Promoting
472 anaerobic co-digestion of sewage sludge and food waste with different types of
473 conductive materials: Performance, stability, and underlying mechanism. Bioresour.
474 Technol., 337, 125384.
475 16. Lin, Q., Li, L., Fang, X., Li, X. 2022. Substrate complexity affects the prevalence
476 and interconnections of antibiotic, metal and biocide resistance genes, integron-integrase
477 genes, human pathogens and virulence factors in anaerobic digestion. J. Hazard. Mater.,
478 438, 129441.
479 17. Lu, T., Zhang, J., Su, T., Liang, X., Wei, Y., He, T. 2022a. Coupled mechanism of
480 enhanced and inhibitory effects of nanoscale zero-valent iron on methane production and
481 antibiotic resistance genes in anaerobic digestion of swine manure. Bioresour. Technol.,
482 360, 127635.
483 18. Lu, Y., Liu, X., Miao, Y., Chatzisymeon, E., Pang, L., Qi, L., Yang, P., Lu, H. 2022b.
484 Particle size effects in microbial characteristics in thermophilic anaerobic digestion of

485 cattle manure containing copper oxide. Environ. Sci. Pollut. Res., 29(42), 62994-63004.
486 19. Pang, L., Xu, K., Qi, L., Chatzisymeon, E., Liu, X., Yang, P. 2022. Response behavior
487 of antibiotic resistance genes to zinc oxide nanoparticles in cattle manure thermophilic
488 anaerobic digestion process: A metagenomic analysis. Bioresour. Technol., 347, 126709.
489 20. Qi, L., Liu, X., Miao, Y., Chatzisymeon, E., Yang, P., Lu, H., Pang, L. 2021. Response
490 of cattle manure anaerobic digestion to zinc oxide nanoparticles: Methane production,
491 microbial community, and functions. J. Environ. Chem. Eng., 9(6), 106704.
492 21. Rivière, D., Desvignes, V., Pelletier, E., Chaussonnerie, S., Guermazi, S.,
493 Weissenbach, J., Li, T., Camacho, P., Sghir, A. 2009. Towards the definition of a core of
494 microorganisms involved in anaerobic digestion of sludge. The ISME Journal, 3(6), 700-
495 714.
496 22. Singh, R., Singh, A.P., Kumar, S., Giri, B.S., Kim, K.H. 2019. Antibiotic resistance
497 in major rivers in the world: A systematic review on occurrence, emergence, and
498 management strategies. J. Cleaner Prod., 234, 1484-1505.
499 23. Tandishabo, K., Nakamura, K., Umetsu, K., Takamizawa, K. 2012. Distribution and
500 role of *Coprothermobacter* spp. in anaerobic digesters. J. Biosci. Bioeng., 114(5), 518-
501 520.
502 24. Tian, Z., Zhang, Y., Yu, B., Yang, M. 2016. Changes of resistome, mobilome and
503 potential hosts of antibiotic resistance genes during the transformation of anaerobic
504 digestion from mesophilic to thermophilic. Water Res., 98, 261-269.
505 25. Xiong, W., Wang, Y., Sun, Y., Ma, L., Zeng, Q., Jiang, X., Li, A., Zeng, Z., Zhang, T.
506 2018. Antibiotic-mediated changes in the fecal microbiome of broiler chickens define the

507 incidence of antibiotic resistance genes. Microbiome, 6(1), 34.
508 26. Xu, R., Zhang, Y., Xiong, W., Sun, W., Fan, Q., Zhaohui, Y. 2020. Metagenomic
509 approach reveals the fate of antibiotic resistance genes in a temperature-raising anaerobic
510 digester treating municipal sewage sludge. J. Cleaner Prod., 277, 123504.
511 27. Xu, W., Long, F., Zhao, H., Zhang, Y., Liang, D., Wang, L., Lesnik, K.L., Cao, H.,
512 Zhang, Y., Liu, H. 2021a. Performance prediction of ZVI-based anaerobic digestion
513 reactor using machine learning algorithms. Waste Manage., 121, 59-66.
514 28. Xu, Y., Yang, S., You, G., Hou, J. 2021b. Attenuation effects of iron on dissemination
515 of antibiotic resistance genes in anaerobic bioreactor: Evolution of quorum sensing,
516 quorum quenching and dynamics of community composition. J. Hazard. Mater., 416,
517 126136.
518 29. Yang, G., Wang, J. 2022. Enhanced antibiotic degradation and hydrogen production
519 of deacetoxycephalosporin C fermentation residue by gamma radiation coupled with nano
520 zero-valent iron. J. Hazard. Mater., 424, 127439.
521 30. Yang, Y., Yang, F., Huang, W., Huang, W., Li, F., Lei, Z., Zhang, Z. 2018. Enhanced
522 anaerobic digestion of ammonia-rich swine manure by zero-valent iron: With special
523 focus on the enhancement effect on hydrogenotrophic methanogenesis activity. Bioresour.
524 Technol., 270, 172-179.
525 31. Yang, Z., Xu, X., Guo, R., Fan, X., Zhao, X. 2015. Accelerated methanogenesis from
526 effluents of hydrogen-producing stage in anaerobic digestion by mixed cultures enriched
527 with acetate and nano-sized magnetite particles. Bioresour. Technol., 190, 132-139.
528 32. Yoo, K., Yoo, H., Lee, J., Choi, E.J., Park, J. 2020. Exploring the antibiotic resistome

529 in activated sludge and anaerobic digestion sludge in an urban wastewater treatment plant
530 via metagenomic analysis. Journal of Microbiology, 58(2), 123-130.
531 33. Zhang, B., Fu, Y., Wang, F., Yang, J., Pan, Z., Huang, M., Shen, K., Shen, C. 2022a.
532 Multidrug-resistant enteroaggregative *Escherichia coli* (EAEC) enters dormant state
533 during heat treatment: A potential hazard in municipal sludge. Environ. Pollut., 305,
534 119312.
535 34. Zhang, J., Sui, Q., Zhong, H., Meng, X., Wang, Z., Wang, Y., Wei, S. 2018. Impacts
536 of zero valent iron, natural zeolite and Dnase on the fate of antibiotic resistance genes
537 during thermophilic and mesophilic anaerobic digestion of swine manure. Bioresour.
538 Technol., 258, 135-141.
539 35. Zhang, T., Yang, Y., Pruden, A. 2015. Effect of temperature on removal of antibiotic
540 resistance genes by anaerobic digestion of activated sludge revealed by metagenomic
541 approach. Appl. Microbiol. Biotechnol., 99(18), 7771-7779.
542 36. Zhang, T., Zhang, X.X., Ye, L. 2011. Plasmid metagenome reveals high levels of
543 antibiotic resistance genes and mobile genetic elements in activated sludge. PLoS One,
544 6(10).
545 37. Zhang, W., Gao, J., Duan, W., Zhang, D., Jia, J., Wang, Y. 2020. Sulfidated nanoscale
546 zero-valent iron is an efficient material for the removal and regrowth inhibition of
547 antibiotic resistance genes. Environ. Pollut., 263, 114508.
548 38. Zhang, X., Li, R. 2020. Variation and distribution of antibiotic resistance genes and
549 their potential hosts in microbial electrolysis cells treating sewage sludge. Bioresour.
550 Technol., 315, 123838.

551 39. Zhang, Z., Li, X., Liu, H., Zamyadi, A., Guo, W., Wen, H., Gao, L., Nghiem, L.D.,
552 Wang, Q. 2022b. Advancements in detection and removal of antibiotic resistance genes
553 in sludge digestion: A state-of-art review. Bioresour. Technol., 344, 126197.
554 40. Zhang, Z., Zhang, Q., Wang, T., Xu, N., Lu, T., Hong, W., Penuelas, J., Gillings, M.,
555 Wang, M., Gao, W., Qian, H. 2022c. Assessment of global health risk of antibiotic
556 resistance genes. Nat. Commun., 13(1), 1553.
557 41. Zhao, X., Liu, M., Yang, S., Gong, H., Ma, J., Li, C., Wang, K. 2022. Performance
558 and microbial community evaluation of full-scale two-phase anaerobic digestion of waste
559 activated sludge. Sci. Total Environ., 814, 152525.
560 42. Zhong, Y., He, J., Zhang, P., Zou, X., Pan, X., Zhang, J. 2022. Effects of different
561 particle size of zero-valent iron (ZVI) during anaerobic digestion: Performance and
562 mechanism from genetic level. Chem. Eng. J., 435, 134977.

563 **Figure Captions**

564 **Figure 1 (**a) Overview profile of antibiotic resistance gene (ARG) types (inner nodes)
565 and their subtypes (outer nodes). (b) Distribution of ARG types in raw sludge (Raw) and
566 sludge treated by thermophilic anaerobic digestion with mZVI at 0 (Z0), 25 (Z1), 100
567 (Z2), 250 (Z3) mg/g TS. Numbers in parentheses on the vertical axis present the number
568 of subtypes affiliated with ARG types, and those on the horizontal axis presents the total
569 abundance (×/Gb) of ARGs in corresponding samples. (c) Shared and unique ARG
570 subtypes. Numbers in parentheses were the total number of ARG subtypes in
571 corresponding samples.

572 **Figure 2** The distribution of antibiotic resistance genes (ARGs) at risk. Q1, Q2, Q3, and
573 Q4 were four levels of health risk posed by ARGs, and Q1 presents the highest risk. Raw:
574 raw sludge; Z0, Z1, Z2, and Z3: samples after digestion with 0, 25, 100, and 250 mg
575 mZVI/g TS.

576 **Figure 3** Overview profiles of microbial (a) composition at the phylum level with (b-f)
577 predominant genera in the top 5 phyla, and relative abundance distribution of (g) all phyla
578 and (h) genera in raw sludge (Raw) and sludge treated by thermophilic anaerobic
579 digestion with mZVI at 0 (Z0), 25 (Z1), 100 (Z2), 250 (Z3) mg/g TS. Others: (a-g) phylum
580 and genus (in its corresponding phylum) with relative abundance < 1.0% and (h) genus
581 with relative abundance < 0.3%. Unclassified: (a-g) unclassified phylum and genus (in its
582 corresponding phylum) with relative abundance > 1.0% and (h) unclassified genus with
583 relative abundance > 0.3%.

584 **Figure 4** (a) Composition of human pathogenic bacteria (top 30 in average relative

585 abundance) in samples before and after digestion. Co-occurrence patterns (R>0.85,
586 p<0.05) between antibiotic resistance gene (ARG) subtypes at high risk and predominant
587 genera (b) (relative abundance > 0.3%), and human pathogenic bacteria (c). The size of
588 each node is proportional to the connection numbers. The edges present the correlation
589 between two nodes. Raw: raw sludge before digestion; Z0, Z1, Z2, and Z3: samples after
590 digestion with 0, 25, 100, and 250 mg mZVI/g TS.

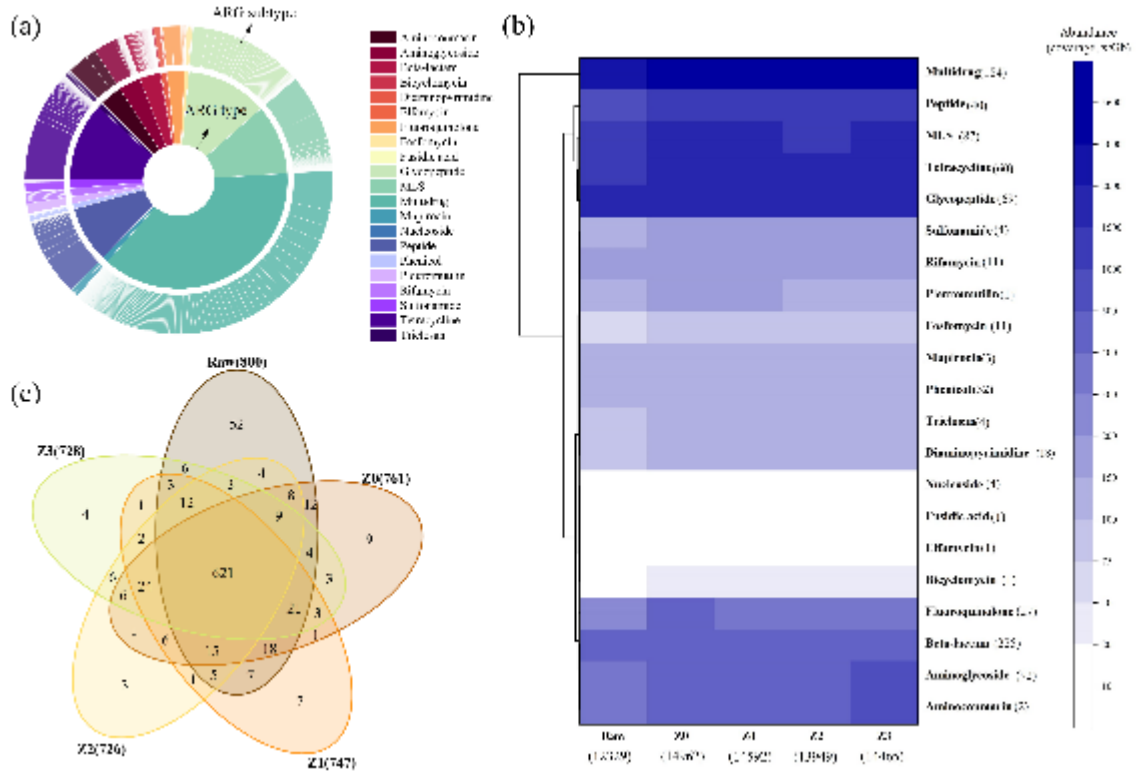

591

592 **Figure 1**

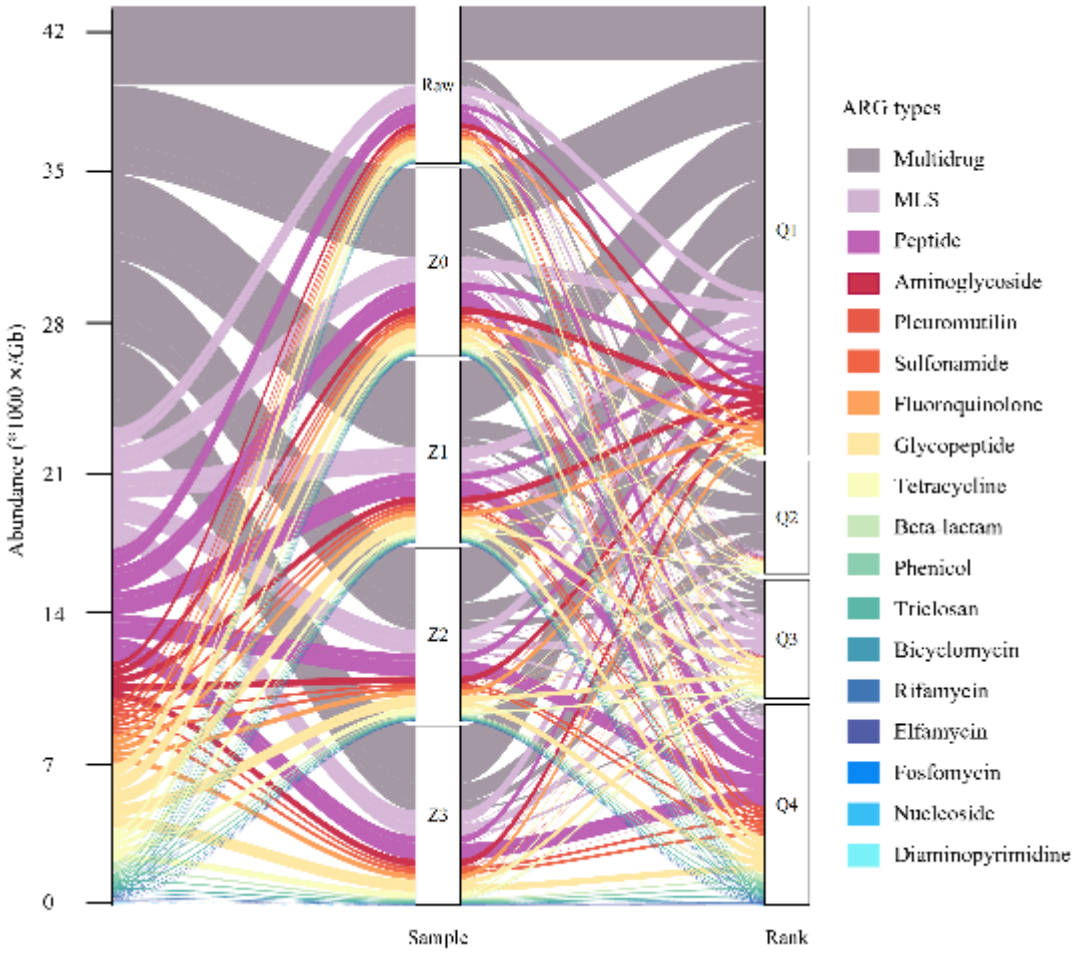

593

594 **Figure 2**

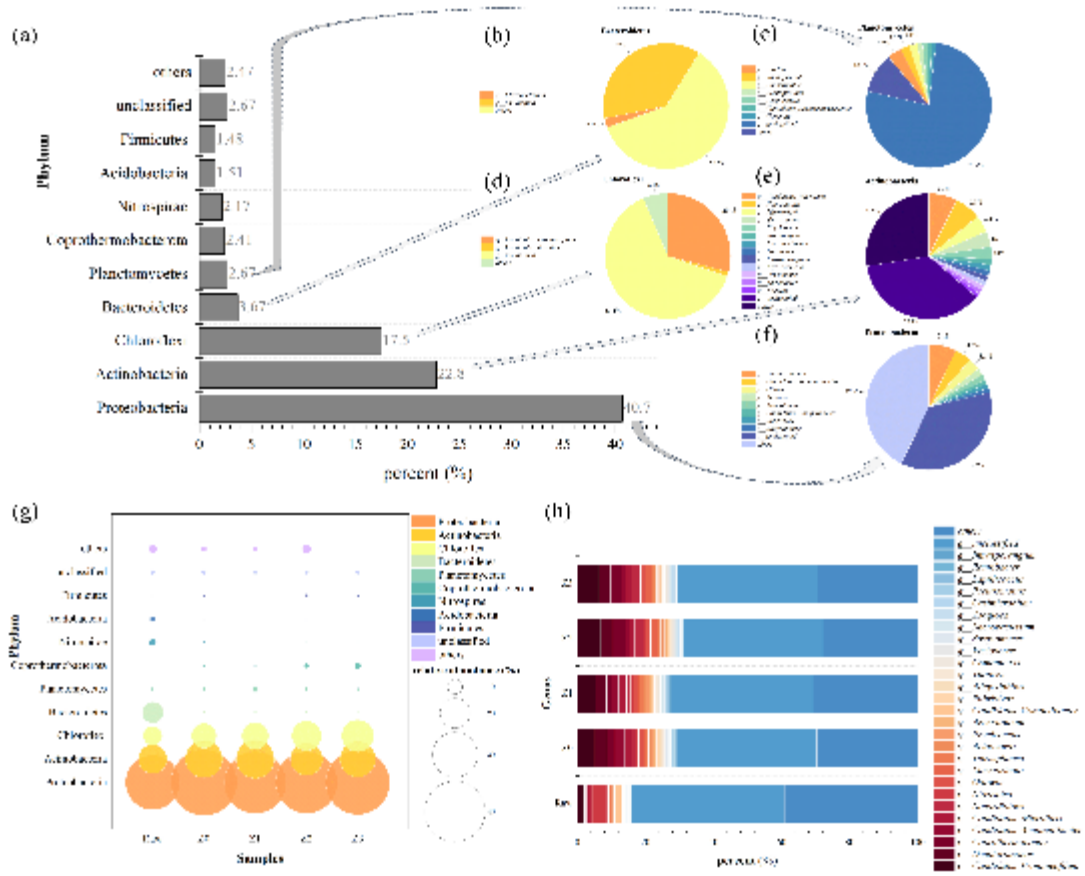

595

596 **Figure 3**

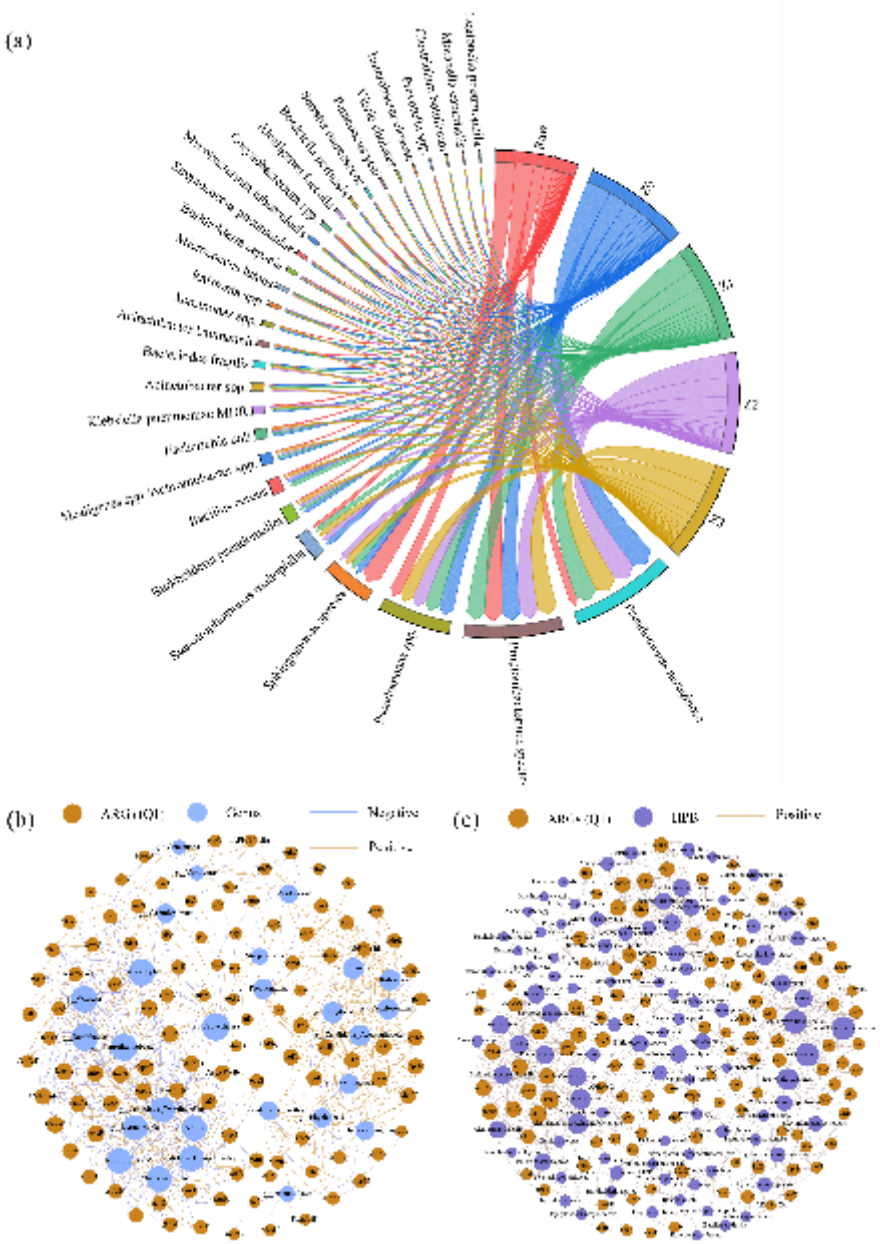

Figure 4

599 **Table 1** Characterization of biogas and methane productions, and raw waste activated sludge before and after 32-day thermophilic anaerobic

600 digestion with different dosages of micron zero valent iron (mZVI).

Parameter	Raw	Z0	Z1	Z2	Z3
Cumulative methane yield (mL/g TS added)	N.A.	2.8 ±0.9^{a}	4.9 ±1.8^{a}	34.1 ±6.1^{b}	34.4 ±6.6^{b}
Cumulative biogas yield (mL/g TS added)	N.A.	34.4 ±0.3^{a}	36.5 ±0.3^{a}	78.7 ±2.4^{b}	80.6 ±2.6^{b}
Total solids (% mass ratio)	26.9 ±2.5^{a}	26.0 ±2.1^{ab}	25.3 ±1.2^{abc}	22.7 ±1.3^{bc}	22.5 ±1.5^{c}
Volatile solids (% mass ratio)	21.4 ±2.5^{a}	20.8 ±1.7^{ab}	20.3 ±1.9^{ab}	17.3 ±2.1^{b}	17.3 ±1.4^{b}
Soluble chemical oxygen demand (mg/L)	2241.0 ±21.2^{a}	12452.5 ±53.0^{d}	13650.0 ±56.6^{e}	10480.0 ±70.7^{b}	11247.5 ±159.1^{c}
Soluble proteins (mg COD/L)	1615.0 ±433.0^{a}	1852.4 ±99.9a^{b}	1721.4 ±115.8^{ab}	2104.4 ±96.1^{b}	1908.9 ±100.7^{ab}
Soluble polysaccharides (mg COD/L)	381.1 ±26.3^{c}	290.1 ±31.4^{b}	381.9 ±25.4^{c}	281.0 ±17.8^{b}	129.6 ±13.6^{a}
Ammonium-nitrogen (mg /g TS added)	1.2 ±0.0^{a}	16.0 ±0.3^{b}	17.8 ±0.7^{c}	19.5 ±1.3^{d}	19.1 ±0.8^{cd}
Acetic acid (mg COD/L)	50.1 ±0.5^{a}	4316.4 ±2.3^{d}	4606.6 ±1.7^{e}	1046.5 ±0.6^{c}	774.3 ±0.8^{b}
Propionic acid (mg COD/L)	14.5 ±0.1^{a}	504.5 ±0.6^{d}	479.7 ±0.4^{c}	472.2 ±0.5^{b}	548.4 ±0.7^{e}
Butyric acid (mg COD/L)	9.7 ±0.0^{a}	147.9 ±0.1^{d}	176.2 ±0.1^{e}	105.1 ±0.1^{c}	81.6 ±0.1^{b}
Iso-butyric acid (mg COD/L)	3.0 ±0.0^{a}	277.6 ±0.0^{b}	286.6 ±0.1^{c}	307.4 ±0.1^{d}	348.2 ±0.1^{e}

Total volatile fatty acids (mg COD/L)	77.2 ±0.6[a]	5246.4 ±3.0[d]	5549.0 ±2.3[e]	1931.1 ±1.3[c]	1752.6 ±1.7[b]
pH	6.6 ±0.0[a]	6.5 ±0.1[a]	6.9 ±0.1[b]	8.4 ±0.1[c]	8.6 ±0.1[d]
Total soluble iron (μg/mL)	0.5±0.0[a]	1.5 ±0.0[b]	2.4 ±0.1[c]	5.9 ±0.1[e]	4.3 ±0.1[d]
Ferrous iron (μg/mL)	0.3 ±0.0[a]	1.4 ±0.0[b]	2.1 ±0.1[c]	5.5 ±0.1[e]	3.9 ±0.1[d]

601 Two samples from each parallel group were analyzed twice.

602 a, b, c, d, e present various significant differences among groups ($p < 0.05$).

603 N.A.: not available; TS: total solids; COD: chemical oxygen demand.